Сибирское отделение Академии наук России

ИНСТИТУТ ЯДЕРНОЙ ФИЗИКИ им.Г.И. Будкера

A.Bondar , A.Buzulutskov, L.Shekhtman, A.Sokolov ,
A.Tatarinov , R.Bellazzini, A.Brez, G.Gariano, L.Latronico,
R.Loni, N.Lumb, M.M.Massai, A.Moggi, G.Spandre

TRACKING PROPERTIES OF THE TWO-STAGE

GEM / MICRO-GROOVE DETECTOR

Novosibirsk
1999

Tracking properties of the two-stage
GEM / Micro-groove detector

A.Bondar[*], A.Buzulutskov[*], L.Shekhtman[*], A.Sokolov[*], A.Tatarinov[*],
R.Bellazzini[**], A.Brez[**], G.Gariano[**], L.Latronico[**],
R.Loni, N.Lumb[**], M.M.Massai[**], A.Moggi[**], G.Spandre[**]

[*] Institute for Nuclear Physics, 630090 Novosibirsk, Russia

[**] INFN Pisa and University of Pisa
Via Livornese 1291, I-56010 S.Piero a Grado, Pisa, Italy

Abstract

Tracking properties of GEM / Micro-groove detectors have been studied at a 120 GeV muon beam at CERN. Detector efficiency reaches 98% when the signal over noise value is equal to ~17. Spatial resolution as high as 30 μ has been measured using a Ne-DME (40 – 60) gas mixture.

_____

Corresponding author, e-mail: lshekhtm@inp.nsk.su

1. Introduction

The Micro-groove detector, introduced in 98 [1], was one of the series of so called micro-pattern detectors produced with high resolution printed circuit board (PCB) technology. The first gas amplifying structure of this type was invented in 96 at CERN [2] and was called the Gas Electron Multiplier (GEM). GEM is made from a double sided copper-clad 50 μm thick kapton foil where small holes with a diameter of below 100 μm are etched through with a pitch of about 150 μm. High voltage is applied between the two sides of the foil. This structure when put in an appropriate gas mixture works as a distributed gas amplifier for the electrons drifting towards and through the holes in the foil. The Micro-groove detector is made on the basis of a similar foil. The foil is glued on a rigid support (thin epoxy glass) and thin linear grooves are etched through with copper strips on top and at the bottom of the grooves (see Fig.1). Negative potential is applied to the top strips with respect to the bottom ones. Electric field lines are concentrated at the bottom of the grooves near the anode strips where the gas multiplication takes place. The Micro-groove detector can operate with a gas gain of several thousands that allows one to detect minimum ionizing particles with full efficiency.

The use of gas chambers in central tracking systems of LHC (Large Hadron Collider) detectors might be affected by intensive fluxes of heavily ionizing particles produced by hadronic interactions in the detector material [3]. High ionization released in the sensitive volume of the detector can cause transition from proportional gas amplification to streamer mode and subsequent sparking, damaging either the amplifying structure itself or front-end electronics. The danger of sparking induced by heavily ionizing particles imposes a severe limit on the maximum gas gain in the detector. It was found however, that if the amplification is divided into two well separated stages, this limit can be efficiently improved [4]. Recently, two-stage detectors combining the GEM and the Micro-groove detector have been successfully tested in a high-intensity hadron beam; it has been proven that they can sustain high fluxes of heavily ionizing particles without sparking up to gains of 5000 − 7000 [5,6].
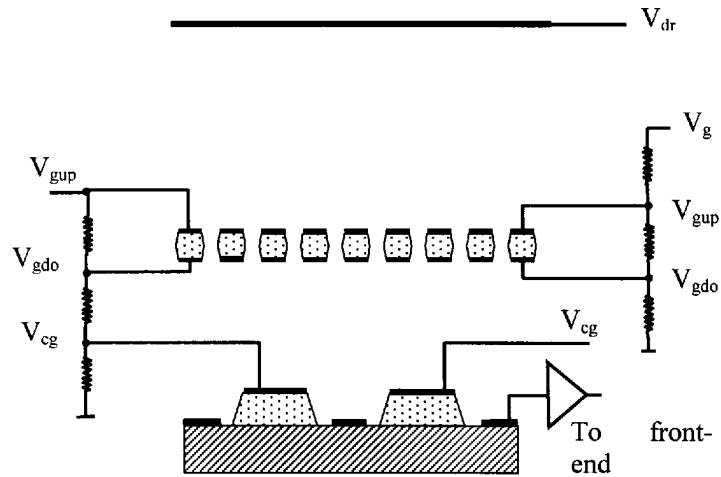
3

Fig. 1. Micro-groove-GEM layout.

In the two-stage system, the electrons first drift through the GEM holes and then across the induction region between the GEM and the Micro-groove detector. Also, the Micro-groove detector has a less compact field in the amplification region compared to some other micro-pattern detectors, for example Micro-strip Gas chambers (MSGC). These factors cause common suspicion that the GEM / Micro-groove detector is slower than MSGC and, with predefined electronics designed for MSGC, needs higher gain to reach the efficiency plateau.

In this work recent results of measurements of efficiency, spatial resolution and timing properties of the GEM / Micro-groove detectors are presented. The measurements were performed in June 99 at CERN, at SPS the X5 beam.

2. Experimental set-up

In the beam test we used two GEM / Micro-groove detectors. The first detector was made in INFN (Pisa) and is called GG20 in the following. The second detector was assembled in BINP (Novosibirsk) and is called WG1. A schematic view of the cross-section of both detectors is shown in Fig.1. The

Micro-groove structures and the GEMs for both detectors were manufactured at CERN. The GEMs are made of 50 μm thick kapton foils with copper on both sides. The holes are etched with a pitch of 140 μm and diameter of 80 μm.

The Micro-groove structure in GG20 has 240 μm pitch, 120 μm wide cathodes and 80 μm wide groove openings at the bottom. The anodes are 30 μm wide. The GG20 length is 250 mm, the width is 110 mm. About 420 anodes are connected to the front-end electronics. The gap between the drift plane and the GEM (drift gap) is 3 mm and between the GEM and the Micro-groove plane (induction gap) is 1 mm. The GEM electrodes along with the Micro-groove cathode are powered through a resistive network. This network consists of 3 equal resistors providing equal voltages to the GEM, induction gap and Micro-groove cathode. The drift electrode is powered through an independent contact.

Detector WG1 has a trapezoidal shape and a wedge structure of grooves. At the wide side the grooves have a 200 μm pitch and at the narrow side the pitch is 180 μm, while the cathode width changes from 120 μm at the wide side to 100 μm at the narrow side. The groove opening is therefore the same along the length of the structure, being equal to 80 μm at the top and 50 μm at the bottom. The anode width is 30 μm. The structure length is 100 mm. 512 anodes are connected to the front-end electronics. The drift and induction gaps are the same in WG1 and GG20. In WG1, the GEM electrodes are powered with the resistive network independently of the Micro-groove detector, unlike in GG20.

The set-up at the SPS X5 beam is shown in Fig.2. The scintillation counters with an active area of 2×2 cm are followed by 4 planes of double side silicon micro-strip telescope called SiBa1,2,3,4. These detectors were used for precise tracking. The distance between the pairs of SiBa1,2 and SiBa3,4 was about 1m. The active area of these detectors was about 2×2 cm. They had 384 channels in each plane with a 50 μm pitch. Between the pairs of telescope planes some other silicon micro-strip detectors were placed. All gas micro-pattern detectors under test were installed behind the last telescope plane. The distance between WG1 and the last telescope plane was about 40 cm. The distance between WG1 and GG20 was 10 cm. GG20 was positioned with strips directed vertically while WG1 had its central strip directed horizontally (see Fig.2, bottom).

The data acquisition system (DAQ) is shown schematically in Fig.3. All detectors were equipped with Premux128 front-end chips [7] which consisted of charge-sensitive amplifiers and shapers with a ~50 ns peaking time. The signal at the output of the shapers could be sampled by sending a «hold» signal at the appropriate moment and stored in an analog buffer. The trigger card formed «hold» signal from the coincidence of two trigger counters. Then «hold» signals were connected to each detector through individual delays adapted to the
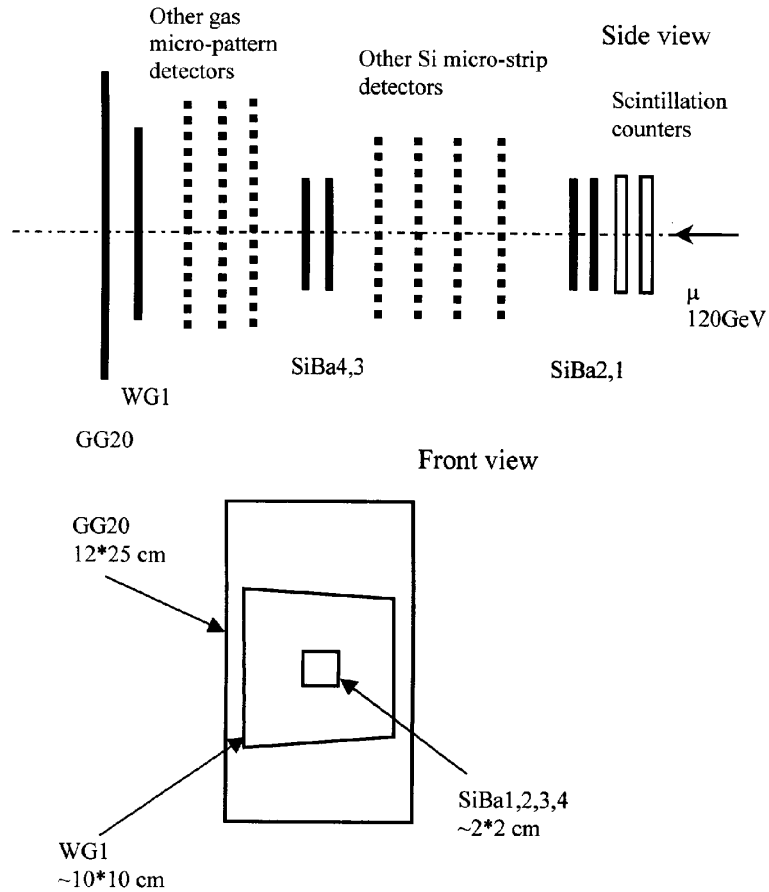
Fig.2. Set-up at X5.

particular pulse shape. By changing this delay we could measure the average pulse shape at the output of the front-end amplifier for a given detector. After the signals are stored in the analog buffer, the control sequence is generated by the sequencer, and all the detectors are simultaneously read-out to the ADCs. All the data were stored in a VME CPU memory and after some reformatting and packaging were sent via a dedicated line to the central computing facilities for subsequent long-term storage.
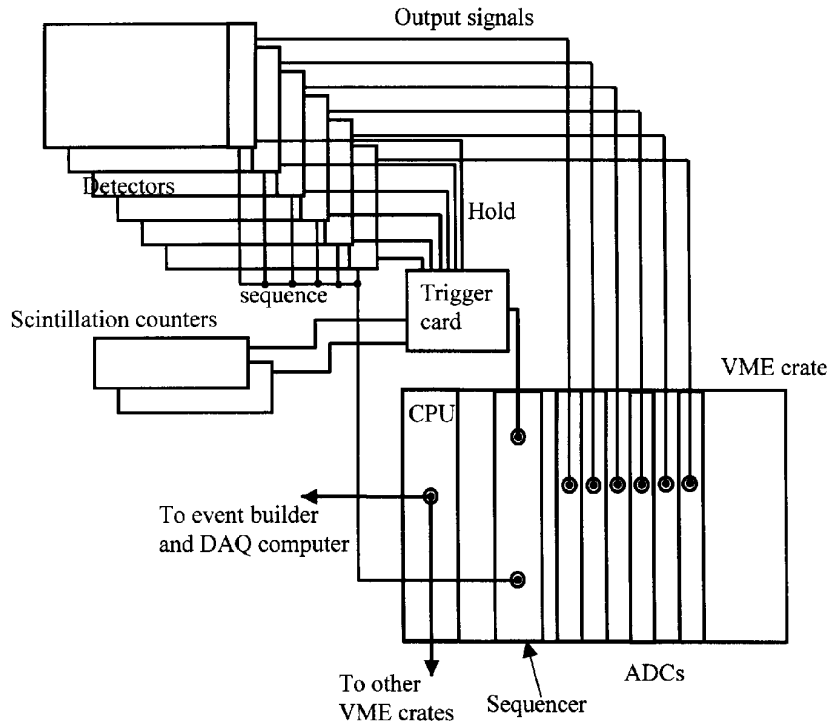
Output signals

Detectors

Hold

sequence

Trigger
card

Scintillation counters

VME crate

CPU

To event builder
and DAQ computer

To other
VME crates

Sequencer

ADCs

Fig. 3. Data Acquisition System.

3. Results and discussion

The algorithm for signal determination, first, selected the channels where the signal over noise ratio exceeded a certain threshold (strip threshold). Then, the signals within continuous groups of such channels (clusters) were summed up. The largest cluster was selected for further analysis if the signal was higher than a certain threshold (cluster threshold). Three planes of silicon telescope (SiBa1, SiBa2, SiBa4) were used for track position reconstruction at the detector plane. Then, the distance between this position and the cluster center of gravity (residual) was determined. This distance was required to be smaller than a certain threshold (corridor). The width of the residuals distribution was minimized using as parameters the inclination of GG20 and WG1 relative to vertical axis, the ratio of the distances GG20-SiBa1 and SiBa1-SiBa4 and a similar ratio for the WG1.

7

For WG1, the correlation between the pitch and horizontal coordinate was taken into account.

The values of strip and cluster thresholds and the corridor were chosen such that, on one hand, the efficiency was stable within some range of threshold and, on the other hand, the probability of ghost clusters was negligible compared to the efficiency. As an example of such analysis we show in Fig.4 the dependence of ghost cluster probability on the width of the corridor. The strip threshold is chosen equal to 3 sigma noise and the cluster threshold is chosen equal to 3 sigma noise quadratically summed over all strips in a cluster. Ghost probability does not increase up to the corridor value of 5 pitches. These particular values of the corridor, strip and cluster thresholds were chosen for further analysis.
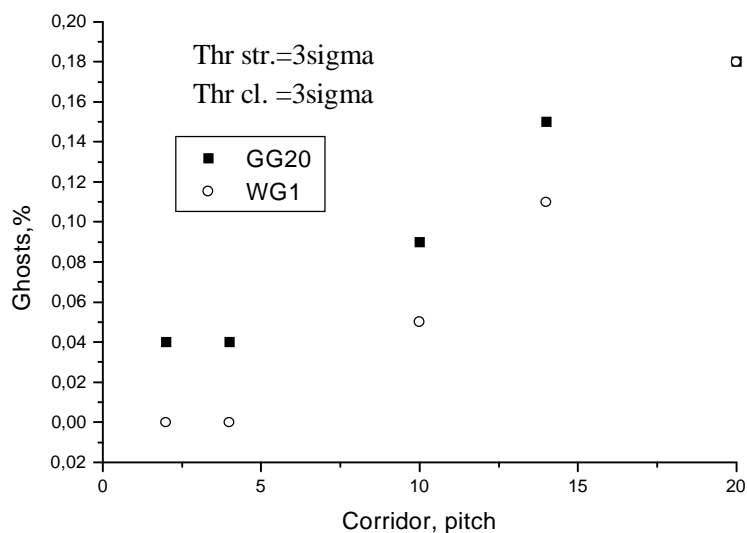
Fig. 4. Justification of the selection algorithm.

As a result of the analysis for each fixed set of parameters (such as voltages, delays, gas mixture etc.), the distributions of signal over noise ratios (S/N), cluster widths, residuals and efficiency were obtained. Here, the notion «signal» means the total signal of a cluster and the notion «noise» means the square average of strip noises over the cluster. From electronic calibration done for WG1, we can derive an approximate relationship between S/N and visible gain of the detector (M): $M \sim 50 S/N$ [6]. For GG20 this relationship is different because the noise is about 50% higher than in WG1 due to the higher strip capacitance. Two examples

8

of such distributions are shown in Fig.5. (S/N distribution for GG20) and Fig.6. (residuals distribution for GG20). Both distributions were obtained at Vcg =Vgdo–Vcg=Vgup–Vgdo=410V (see Fig.1), drift field equal to 9 kV/cm and gas mixture DME-Ne (3–2). The S/N distribution can be fitted with a Landau function with the maximum at ~50. The distribution of residuals has a sigma of ~0.15 (in units of pitch) which corresponds to 38 μm.
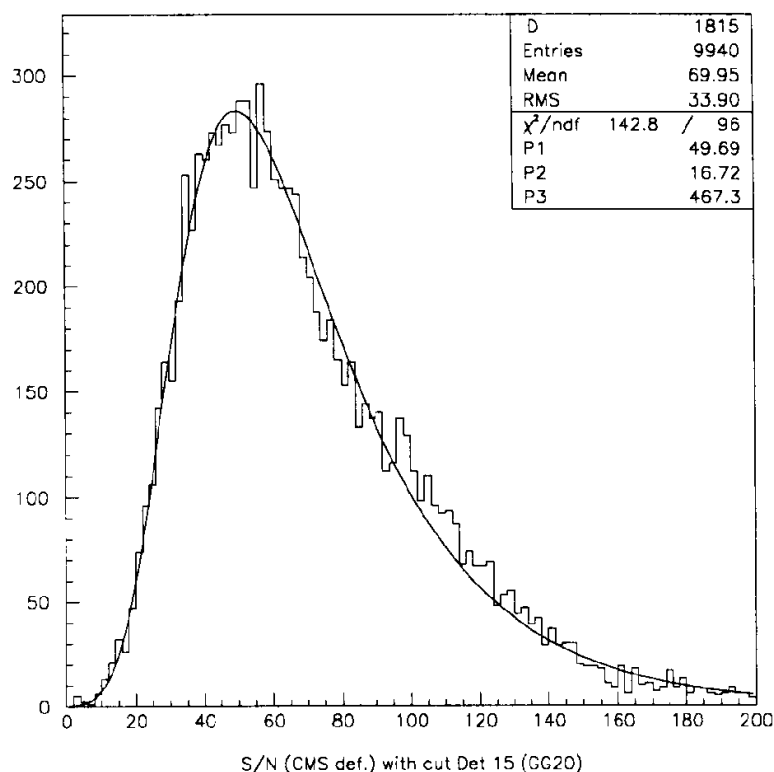
D		1815
Entries		9940
Mean		69.95
RMS		33.90
χ^2/ndf	142.8	/ 96
P1		49.69
P2		16.72
P3		467.3

S/N (CMS def.) with cut Det 15 (GG20)

Fig. 5. Distribution of the signal over noise values for GG20.

The pulse width shape, after the front-end amplifier, was investigated by scanning the signal value as a function of the delay in the «hold» line (delay curve). We were not able to change independently the voltages applied to the GEM, induction gap and Micro-groove cathode, because the appropriate electrodes were powered through a common resistive network. The field in the induction gap of the GG20 was always about 4 kV/cm. In order to investigate the dependence of the pulse width on the field intensity in the induction gap, the

9

resistive network in WG1 was chosen such that this field was much lower than in GG20, namely between 1 kV/cm and 2 kV/cm, depending on a particular voltage applied to the Micro-groove cathode.
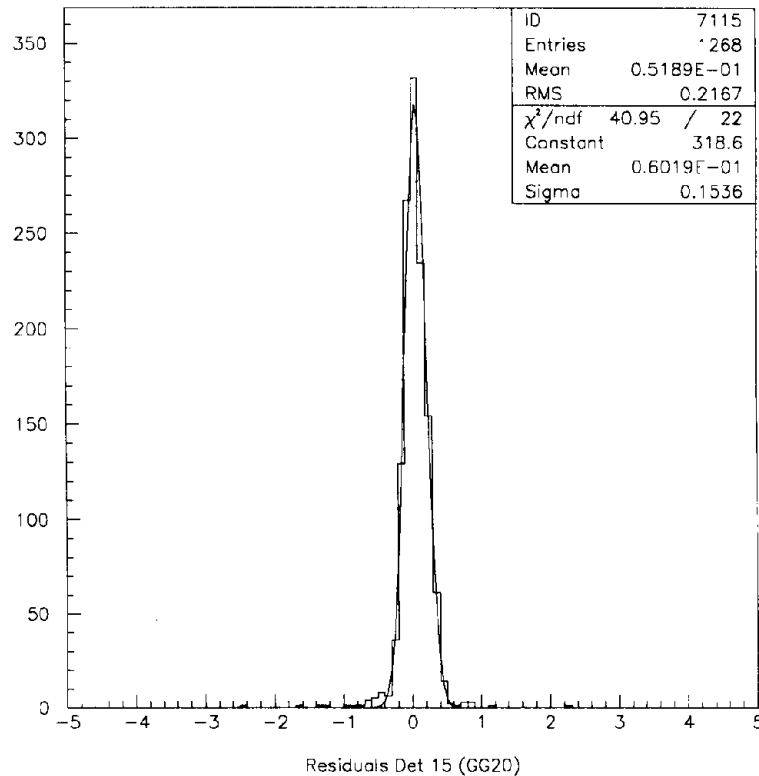
Residuals Det 15 (GG20)

Fig. 6. Distribution of the residuals for GG20.

In Fig.6 the delay curves for WG1 and GG20, at different fields in the drift gaps, are shown for a DME-Ne (3–2) gas mixture. During this measurement, the field in the induction gap of WG1 was about 1.5 kV/cm. Comparing the curves for WG1 at 7 kV/cm drift field and GG20 at 6 kV/cm drift field we see that the pulse shape does not depend on the induction field within the precision of the measurement. The pulse shape changes only when the drift field drops below a certain value, as we can see comparing the measurement for the drift field of 7 kV/cm and 5 kV/cm for WG1. For a mixture with saturated drift velocity such as Ar-CO_2 (70–30), we see neither any essential dependence of the pulse shape on
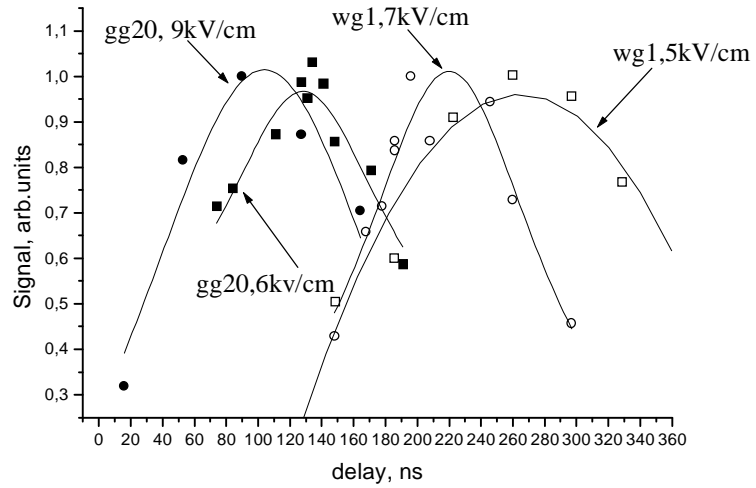
10

Fig. 7. Delay curves for Ne-DME.

the induction field nor any difference in delay between the two detectors (Fig.8). The small difference in the pulse width between WG1 and GG20 can be explained by a lower transverse diffusion in the induction gap of WG1, due to a lower induction field, which then increase slightly in the region of higher fields corresponding to that of GG20.
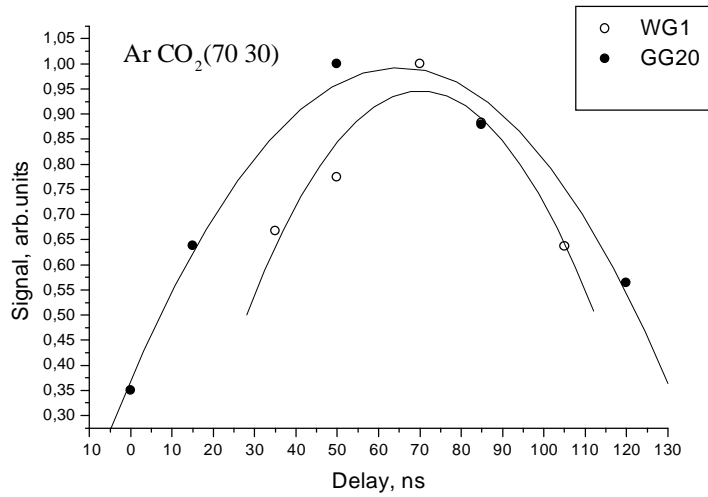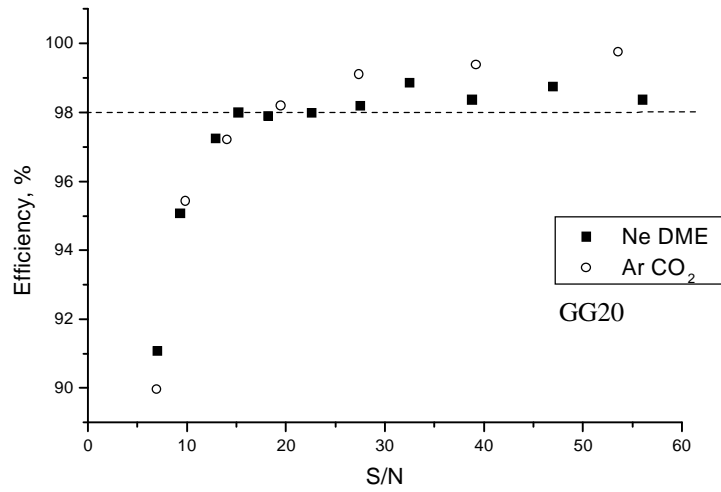

Fig. 8. Delay curves for Ar-CO2.
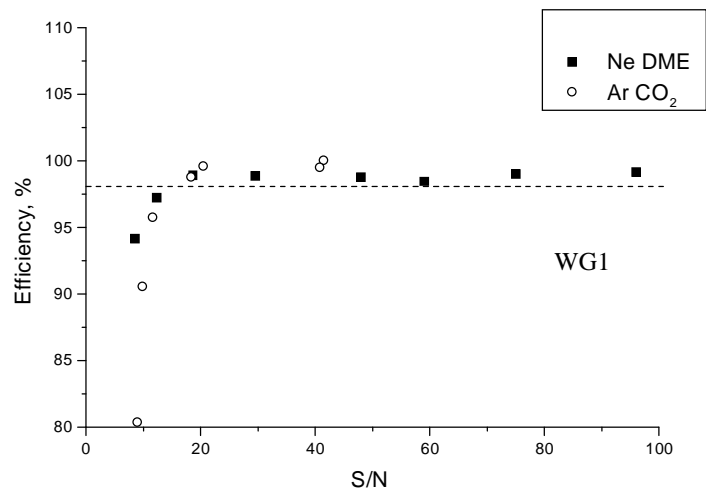
11

Fig. 9. Efficiency vs S/N for GG20.

Fig. 10. Efficiency vs S/N for WG1.

Another important issue for tracking detectors is the particular value of S/N at which the efficiency comes to plateau. This value of S/N is a universal feature of the detector and does not depend on electronics, strip capacitance or other
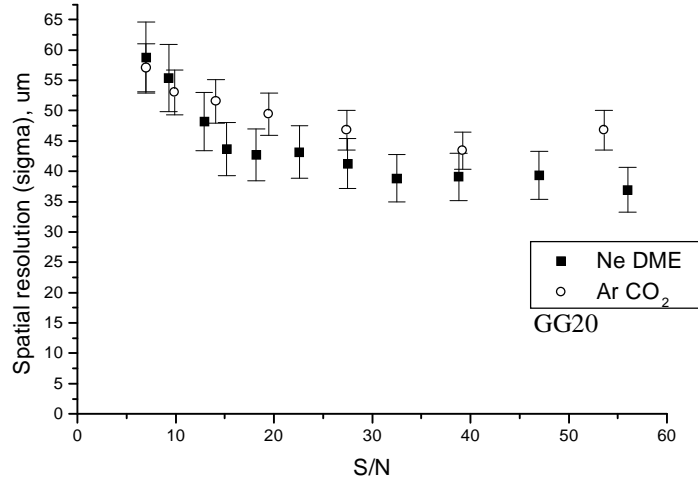
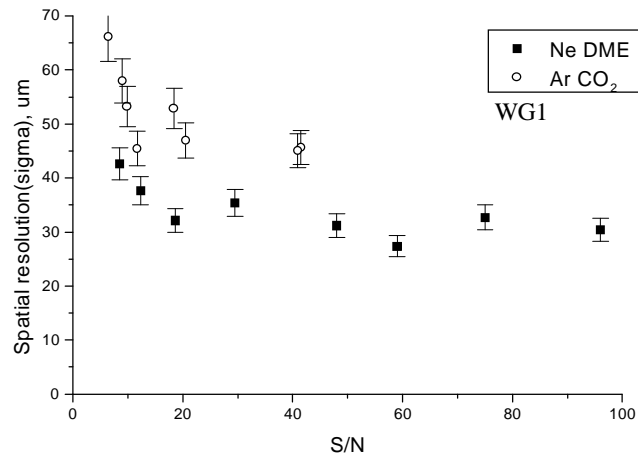*Fig. 11.* Spatial resolution vs S/N for GG20.

Fig. 12. Spatial resolution vs S/N for WG1.

additional noise sources. Additional fluctuations of the signal charge due to the limited transparency of the GEM can affect the width of pulse height distribution and thus the starting point of the efficiency plateau. In Figs.9,10 the efficiency versus S/N dependencies are shown for GG20 and WG1 and for two gas mixtures: DME-Ne (3–2) and Ar-CO_2 (70–30). 98% efficiency is reached in all cases at S/N~17. For a single MSGC this value is about 13 [8]. We see that within the

experimental errors there is no difference between the two gas mixtures and between low and high induction fields. That means that fluctuations of the charge extracted from the GEM hole at low induction field are negligible and do not affect the width of the pulse height distribution.

The dependencies of sigma of the gaussian fit to the track residuals distribution on S/N, for two detectors and different gas mixtures, are shown in Fig.11,12. The spatial resolution in all cases improves with S/N and comes to plateau at S/N~20. For the Ar-CO_2 mixture the resolution is almost the same for GG20 and WG1 and is equal to ~45 μm. For DME-Ne the resolution is significantly better in the case of the smaller pitch detector (WG1) and is equal to ~30 μm, while for GG20 it equals ~40 μm. This difference can be explained by the larger cluster width in the case of the Ar-CO_2 mixture that can be observed in Fig.13 for WG1 and in Fig.14 for GG20. This larger size is mainly caused by the longer range of delta electrons in the Ar-based mixture compared to the DME-based one. Thus the cluster position fluctuates more for the Ar-CO_2 mixture. The cluster width for the Ar-CO_2 mixture is significantly larger than the pitch for both detectors; it determines the resolution. For the DME-Ne mixture the cluster width is already comparable to the pitch and therefore the dependence on pitch is well pronounced.
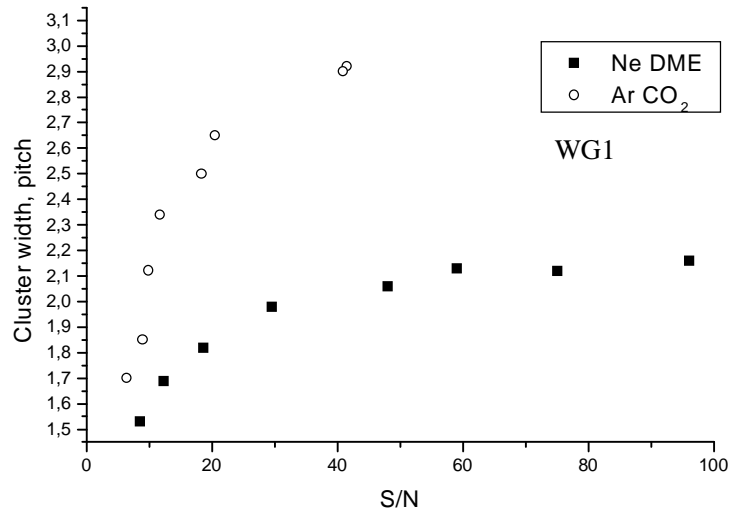

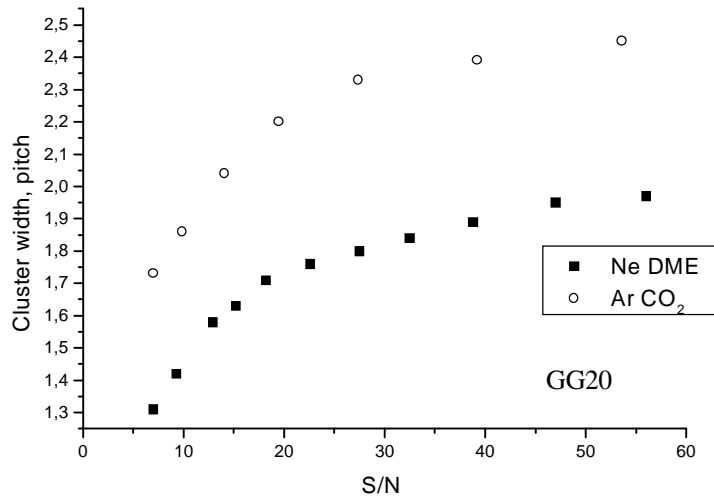Fig. 13. Cluster width vs S/N for GG20.

Fig. 14. Cluster width vs S/N for WG1.

4. Conclusions

Two GEM / Micro-groove detectors have been tested in a 120 GeV muon beam at CERN. The major properties of these detectors for localization of tracks of minimum ionizing particles have been investigated.

We found that the signal pulse width does not depend on the electric field in the induction gap (induction field). The only timing parameter that changes with the induction field is the arrival time of the signal. The pulse width depends however on the electric field in the drift gap.

The detector efficiency reaches 98% at a signal over noise ratio of ~17. This value does not change with the induction field and the gas mixture. Notice that for a single MSGC, 98% efficiency is achieved at S/N~13 [8]. Thus, we may conclude that some additional fluctuation of the gain is contributed by the GEM. However this effect is not very large.

The spatial resolution of the detectors reaches a plateau at S/N~20. While in Ar-CO_2 the spatial resolution does not depend on the pitch and is equal to ~45 μm, in Ne-DME it is significantly better due to more compact charge clusters

15

with higher primary electron statistics and amounts to ~40 μm and ~30 μm for the pitch of 240 μm and 190 μm respectively.

References

[1] R.Bellazzini et.al., Nucl.Instr.& Meth. A424 (1999), 444.

[2] R.Bouclier, M.Capeans, W.Dominik, M.Hoch, J-C.Labbe, G.Million, L.Ropelewski, F.Sauli and A.Sharma, The Gas Electron Multiplier (GEM), CERN-PPE/96-177, Presented at the IEEE NS Simposium, Anaheim, November 1996.

[3] M.Huhtinen, CMS Note-1997/073, CERN, Geneva, 1997.

[4] A.Bressan et.al. Nucl.Instr.& Meth. A424 (1999), 321.

[5] R. Bellazzini, A. Brez, G. Gariano, L. Latronico, R. Loni, N. Lumb, A. Moggi, A. Papanestis, S. Reale, G. Spandre, M.M. Massai, M.A. Spezziga, A. Toropin, Tests of a Micro-Groove Detector coupled to a GEM in a high-intensity hadron beam, Presented at The International Workshop on Gas Micro-pattern detectors, Orsay, June 1999.

[6] A.Bondar, A.Buzulutskov, L.Shekhtman, A.Sokolov, A.Tatarinov, Experience with wedge MSGC-GEM and wedge Micro-groove-GEM structures in high intensity hadron beam, Presented at The International Workshop on Gas Micro-pattern detectors, Orsay, June 1999.

[7] L.Jones, PreMUX128 specification Vsn 2.3 Rutherford Appleton Laboratory internal document (1995).

[8] CMS, The Tracker Project, Technical Design Report, CERN-LHCC/98-6, Geneva, 1998.